Available online at www.sciencedirect.com
SCIENCE DIRECT®
Applied Geochemistry 20 (2005) 1658–1676
Applied Geochemistry
www.elsevier.com/locate/apgeochem

Groundwater recharge, circulation and geochemical evolution in the source region of the Blue Nile River, Ethiopia

Seifu Kebede [a,b,*], Yves Travi [a], Tamiru Alemayehu [b], Tenalem Ayenew [b]

[a] *Laboratory of Hydrogeology, University of Avignon, 33 Rue Louis Pasteur, 84000 Avignon, France*
[b] *Department of Geology and Geophysics, Addis Ababa University, P.O. Box 1176, Addis Ababa, Ethiopia*

Received 3 February 2004; accepted 20 April 2005
Editorial handling by W.M. Edmunds

Abstract

Geochemical and environmental isotope data were used to gain the first regional picture of groundwater recharge, circulation and its hydrochemical evolution in the upper Blue Nile River basin of Ethiopia. Q-mode statistical cluster analysis (HCA) was used to classify water into objective groups and to conduct inverse geochemical modeling among the groups. Two major structurally deformed regions with distinct groundwater circulation and evolution history were identified. These are the Lake Tana Graben (LTG) and the Yerer Tullu Wellel Volcanic Lineament Zone (YTVL). Silicate hydrolysis accompanied by CO_2 influx from deeper sources plays a major role in groundwater chemical evolution of the high TDS *Na–HCO₃* type thermal groundwaters of these two regions. In the basaltic plateau outside these two zones, groundwater recharge takes place rapidly through fractured basalts, groundwater flow paths are short and they are characterized by low TDS and are *Ca–Mg–HCO₃* type waters. Despite the high altitude (mean altitude ~2500 masl) and the relatively low mean annual air temperature (18 °C) of the region compared to Sahelian Africa, there is no commensurate depletion in $\delta^{18}O$ compositions of groundwaters of the Ethiopian Plateau. Generally the highland areas north and east of the basin are characterized by relatively depleted $\delta^{18}O$ groundwaters. Altitudinal depletion of $\delta^{18}O$ is 0.1‰/100 m. The meteoric waters of the Blue Nile River basin have higher d-excess compared to the meteoric waters of the Ethiopian Rift and that of its White Nile sister basin which emerges from the equatorial lakes region. The geochemically evolved groundwaters of the YTVL and LTG are relatively isotopically depleted when compared to the present day meteoric waters reflecting recharge under colder climate and their high altitude.

1. Background

Surface water of the Blue Nile River basin of Ethiopia is not widely used for water supply because of its marked seasonality and lack of proper technology to retain it. In the basin, groundwater is the most important source of water and is the dominant source for domestic supply, especially in the dry areas where surface waters are scarce (UN, 1989). Groundwater well drilling programmes have been initiated over the last decades, but groundwater provision is often unsuccessful because of poor groundwater productivity of wells, difficult drilling conditions, drying of wells and springs after prolonged drought, or sometimes due to poor quality. This is hampered by lack of understanding of groundwater systems. Information on groundwater recharge, storage, circulation, and chemical evolution is barely known. Ground-

* Corresponding author.
E-mail address: Seifu.Kebede@univ-avignon.fr (S. Kebede).

0883-2927/$ - see front matter © 2005 Elsevier Ltd. All rights reserved.
doi:10.1016/j.apgeochem.2005.04.016

water development is being conducted without a good understanding of its role in the hydrology of the basin.

In contrast to the Blue Nile River basin, many important hydrogeochemical researches have been conducted in the Ethiopian Rift System. The presence of many lakes, lacustrine deposits, heat flow owing to Rifting and accompanied thinning of the crust in the East African Rift System (EARS) have attracted major geoscientific investigations since the second half of the 20th century. Many of the geochemical investigations (Craig et al., 1977; Darling, 1996; Darling et al., 1996; Gizaw, 1996; Chernet et al., 2001; Reimann et al., 2003) showed the role of water–rock interaction in influencing the water quality, salinity and F^- composition of groundwaters and thermal systems of the EARS. In many instances the water–rock interaction is induced by volatile gases from the mantle and by the high heat flow beneath the EARS. Groundwater circulation pattern, groundwater recharge source identification and the interaction between lakes and groundwaters have also been the subject of many important studies in the EARS (Schoell and Faber, 1976; Craig et al., 1977; Darling et al., 1996; Ayenew, 1998; McKenzie et al., 2001). Many of these studies show riftward groundwater flow from adjacent highlands. However little is known about the hydrogeology, hydrogeochemistry and isotopic compositions of the groundwaters of the adjacent plateaus to substantiate the hypotheses of the plateau–rift groundwater connections.

Therefore, understanding the hydrogeochemistry, and hydrogeology of the Blue Nile River basin has atleast a twofold importance. The first is directly linked to the understanding of the role of the aquifers of the relatively humid NWP (in which the Blue Nile is a part) in recharging the groundwaters and thermal waters of the arid regions of the Ethiopian Rift. The second is related to groundwater resources assessment in the Blue Nile River basin where clean water provision is still not attained.

This work uses geochemical and isotope hydrological approaches to provide an initial schematic geo-hydrological model on groundwater recharge, circulation, chemical evolution and its subsurface residence time in the poorly known hydrogeologic system of the upper Blue Nile River basin of Ethiopia. The present isotope data are the first set of data ever obtained in the Northwestern Ethiopian Plateau. The specific objectives of this work are: (1) to characterize the isotopic ($\delta^{18}O$, δD, $\delta^{13}C$, ^3H) compositions of the groundwaters of the Blue Nile River basin; (2) to determine sources and mechanisms of recharge of groundwaters in the Blue Nile River basin; (3) to determine the dominant geochemical processes that influence groundwater chemical composition; and, (4) to schematize groundwater flow patterns and the nature of aquifers in selected important hydrogeological regions of the basin.

2. Study site description, geology and hydrogeology

The Blue Nile River basin is located in the Northwestern Ethiopian Plateau. The Main Nile River gets 70% of its flow from the Blue Nile emerging from the Ethiopian Plateau and the remaining from the White Nile emerging from the Equatorial Lakes. About 44% of the Ethiopian population lives in the Blue Nile basin (BCEOM, 1999). The basin has an elevation ranging from 500 m in the western lowland to over 4000 m in the east and northeast. Spatial variation in rainfall amount is controlled by topography. Annual rainfall varies between 1000 mm in the lowland to 2000 mm in the highland. The Atlantic Ocean is the main source of rainfall in summer (June, July, August and September). The eastern mountainous region of the basin receives rainfall originating from the Indian Ocean in April and March.

2.1. Geology

The geology of the Blue Nile basin has been studied by various authors (Yemane et al., 1985; Assefa, 1991; Abate et al., 1996; Abebe et al., 1998; Chorowiz et al., 1998; Pik et al., 1998; Kebede et al., 1999; Asrat et al., 2001; Feseha, 2002). Crystalline basement rocks, volcanic rocks, and sediments make up the geology of the basin (Fig. 1).

The oldest rocks in the region form the Precambrian basement. They are exposed in the low-lying plain in the western part of the basin. The various rocks forming the basement are broadly classified in to two petrographically and structurally distinct units (Kebede et al., 1999). These are the high grade gneisses and the volcano-sedimentary green schist assemblages with associated ultramafic rocks. The Paleozoic is characterized by erosion and lack of any major rock formation.

Mesozoic sedimentary rocks are exposed in the Blue Nile gorge and the gorges of its major tributaries. The succession is about 1200 m thick. It includes from the bottom to the top, 5 units: lower sandstone (or Adigrat sandstone), the lower muddy sandstone (Gohation formation), Antalo limestone, the upper muddy sandstone (or mugger sandstone and gypsum) and the upper sandstone (Debrelibanos sandstone).

The Cenozoic is characterized by extensive faulting accompanied by widespread volcanic activity and uplift. The outpouring of vast quantities of a basaltic lava accompanied by the eruption of large amounts of ash resulted in a basaltic plateau often called trap series basalts. Several shield volcanoes, also consisting of alkali basalts and fragmental material, cover the center and the upper part of the Blue Nile basin. Over two third of the upper Blue Nile is covered by Cenozoic basalts and ashes. The mineralogical compositions of the basalts are spatially variable but all the basalt types contain

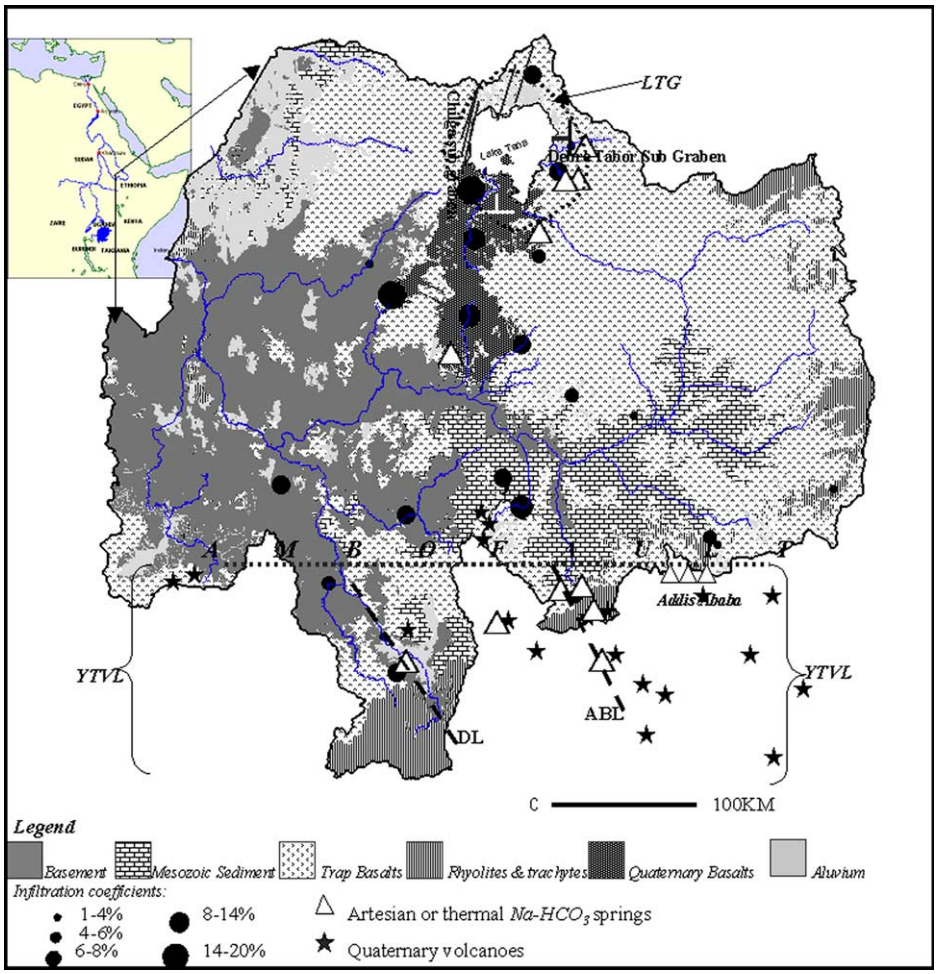

Fig. 1. Simplified geological and hydrogeological map of the Blue Nile basin (Modified from Abebe et al., 1998, Chorowiz et al., 1998, and BCEOM, 1999). The western part of the LTG (Chilga sub graben) is highly faulted. Rock blocks dipping inward towards lake Tana are common around the lake. The zone bounded by the big bracket is the YTVL The prominent features of the YTVL are the Ambo fault which makes the northern boundary of the YTVL and the two NW–SE transfer zones DL (Didesa Line) and the ABL (Ambo-Butajira Line). Thermal spring sites and Quaternary volcanoes are almost exclusively located in the LTG and YTVL. The Quaternary basalts south of lake Tana have the highest infiltration coefficient and metamorphic basement has the lowest infiltration coefficient.

dominantly olivines and clinopyroxenes with minor but variable amounts of plagioclase, K–feldspars, and brown glass (Pik et al., 1998). The K–feldspars and brown glass are abundant in basalts of the southern sector of the plateau and plagioclase dominates in the basalts of the western and northern sectors. Quaternary lacustrine and fluvio-colluvial sediments and superficial deposits occur intermittently covering the basement and filling river channels.

There are two prominent tectonically deformed regions on the plateau. These are the Lake Tana Graben (LTG) and the Yerer-Tullu Wellel Volcanic Lineament zone (YTVL). The majority of the geothermal springs, Quaternary volcanoes, and quaternary basalt flows that exist in the Blue Nile basin are located in these two zones. These tectonic structures play an important role in controlling groundwater flow paths and groundwater chemical evolution. Although the groundwater flow conditions, the recharge conditions, and groundwater origin were unknown, the YTVL and the LTG were previously identified as a potential site of low enthalpy geothermal energy (Abebe, 2000). This observation was based on the presence of favorable geological structures, rainfall amount and heat flow.

The LTG is a circular depression characterized by faulted blocks dipping towards lake Tana from all directions (Fig. 1). The faulted blocks in the western part of the lake have an average width of 1–4 km and strike

NNE-SSW. Gently inward-directed dips of the Tertiary basalt toward the center of the Tana basin are present to the west, north and east of the lake. In eastern (Debertabor subgraben) and the north western (Chilga subgraben) subcatchments of the LTG, the late Miocene ligniteferous lacustrine deposits exist embedded in the trap series basalts (Chorowiz et al., 1998; Feseha, 2002). The Miocene lacustrine deposits contain mainly reworked volcaniclastics, thin layers of lignites, claystones, and siltstones. In places these sediments may have a thickness of 130 m. Basaltic volcanism continued in the region until 10 ka and basaltic lava covers the Miocene sediments.

The YTVL is an east–west trending zone that partly crosses the Blue Nile basin. It has a length of 800 km and a diameter of 80 km. The YTVL is a kind of half graben bounded by the Ambo fault from the north (Abebe et al., 1998). The Ambo fault has a throw of about 500 m. The major lineaments in the YTVL zone are the Didesa Lineament (DL) and the Ambo-Butajira Lineament (ABL). These lineaments are deep faults that cut across the YTVL. Along the YTVL, 3 main rock successions crop out: the Precambrian basement, the Mesozoic sedimentary rocks, and the Cenozoic volcanics. The volcanics are predominant whereas the basement and the sedimentary rocks are locally exposed. The sedimentary rocks (sandstones and limestones) thin out towards the southern part of YTVL. The Quaternary volcanics which cover the YTVL are mainly rhyolites and trachytes with abundant alkali–feldspars, alkali amphiboles and quartz. Faulting in the YTVL (the Ambo fault and associated lineaments) for instance juxtaposes the Mesozoic sediments and the volcanic cover favoring the formation of high discharge, low temperature thermal springs in the region.

2.2. Hydrology and hydrogeology

The Blue Nile drainage is the result of river incision of the Cenozoic basaltic uplifted land. The Blue Nile River captures much of its runoff from the highlands in the southern and central part of the basin. The Blue Nile River is characterized by very high discharge during the wet season and very low discharge during the dry season. This reflects that the river discharge is dominated by inputs from rainfall and surface runoff rather than groundwater.

With the exception of the eastern sector of the basin just east of the water divide of the Blue Nile basin where thick intermountain alluvial sediments bear high groundwater yield, the majority of groundwaters in the Blue Nile basin are abstracted from the fractured basaltic or metamorphic rocks. The well depth in the basaltic plateau ranges from 30 to 120 m. The majority of cold springs emerge from the basaltic plateau. Because of dissection and fragmentation by river erosion, the basaltic cover is considered to be perched groundwater systems with low storage and small aerial extent (BCEOM, 1999). Hydrograph separation shows that infiltration coefficient ranges from 3% to 20% of the total rainfall in the basaltic plateau (BCEOM, 1999). The highest infiltration coefficient and the highest groundwater contribution to surface water occur in the central Gojam highland region surrounding the Choke shield volcano and in the Lake Tana Graben. High rainfall on the shield volcano and the large lateral extent of the aquifers in that part of the plateau favors good groundwater storage in that region. Three high discharge springs: the Bure Baguna Springs, the Andesa high TDS springs, and the Jiga low TDS springs emerge at the foot of the shield volcano. Regions on the left bank, particularly the eastern and the south-eastern part of the Blue Nile River have generally low infiltration coefficient and low groundwater storage. This is most likely because of the strong dissection and fragmentation of the aquifers and the low rainfall in this part of the basin. Generally the Mesozoic sedimentary formations are thought to be good aquifers (BCEOM, 1999). The Mesozoic sediments, however, are only locally exposed. The relatively low infiltration coefficient in the southwestern part of the basin is related to the low permeability of the basement rock underlying that region.

The few pumping test data (BCEOM, 1999) in the region shows that the transmisivity is highly variable ranging from 1 to 700 m^2/day. The Quaternary basalts surrounding Lake Tana are characterized by high transmisivity (100–200 m^2/day) compared to the basalts of the trap series. Quaternary alluvial sediments have the highest transmisivity (in places more than 700 m^2/day). The metamorphic rocks in the western lowland have the lowest transmisivity (as low as 1 m^2/day).

3. Methodology and materials

The methods used to achieve the objectives includes: (a) direct analysis of the raw isotope hydrological and geochemical data; (b) statistical classification of the data set accompanied by associating the statistical classes of the waters with hydrogeological variables; and, (c) geochemical modeling. Furthermore $\delta^{13}C$, P_{CO_2}, pH and carbonate species compositions of the groundwaters were used to gain additional insight on groundwater geochemical evolution.

3.1. The chemical and environmental isotope data

The majority of the water samples were collected from the upstream part of the Blue Nile River basin (Fig. 2). A total of 140 water samples were collected from groundwater wells, springs, lakes and rivers between November 2001 and August 2002. The samples

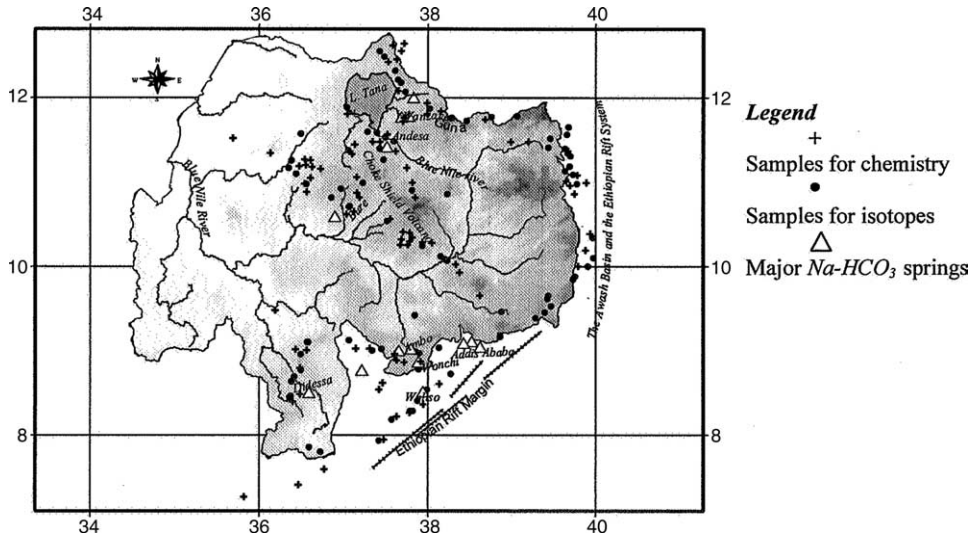

Fig. 2. Location map of water sampling points and other important sites. The region south of the Ethiopian rift margin is the Main Ethiopian Rift. Names of some localities are also shown.

were analyzed for their major ion concentrations as well as for their isotope contents ($\delta^{18}O$, δD). Selected representative groundwater samples were analyzed for $\delta^{13}C$ and ^{3}H at the International Atomic Energy Agency (IAEA) and the University of Avignon, respectively. Chemical analyses were carried out at the Laboratory of Hydrogeology, University of Avignon (France) while isotope compositions were measured at the IAEA Laboratory, Vienna. The $\delta^{18}O$ and δD compositions were reported in ‰ notation calibrated against the V-SMOW. Tritium concentration is reported in tritium units (TU). The $\delta^{13}C$ is reported in ‰ notation calibrated against PDB. Cation species were analyzed using Atomic Absorption Spectrometry. Anion species were analyzed using a Dionex Ion Chromatograph equipped with automatic sampler. Silica (SiO_2) was analyzed using colorimetric methods. Bicarbonate, CO_3^{2-}, pH, and temperature were measured in situ. Missing CO_3^{2-} are estimated from pH and the activity of HCO_3^- using the equation $K_2 = [CO_3^{2-}][H^+]/[HCO_3^-]$. The partial pressure of P_{CO_2} is estimated using the equation $K_{CO_2} = [H_2CO_3]/P_{CO_2}$. Saturation indices were calculated from chemical activities and ionic strength. Thirty two groundwater chemical data points from a previous study (BCEOM, 1999) were included in the data set. The results of the analyses are presented in Appendix 1 (see web version).

3.2. Q-mode statistical cluster analysis

Statistical classification of geochemical data by Q-mode hierarchical cluster analysis (HCA) has proven to provide a suitable basis for objective classification of water composition into hydrochemical facies and for geochemical modeling (Alberto et al., 2001; Barbieri et al., 2001; Meng and Maynard, 2001; Swanson et al., 2001; Güler et al., 2002; Güler and Thyne, 2004). HCA is a semi-statistical technique intended to classify observations (e.g., water chemistry) so that the members of the resulting groups or subgroups are similar to each other and distinct from the other groups. The characteristics of the groups or sub groups are not pre determined but can be obtained after the classification. The results obtained in HCA and the robustness of the HCA are justified according to their values in interpreting the data and in indicating patterns. It is therefore not the number of members of a group that determines the robustness of HCA. It is possible that many single member groups that do not belong to any of the multi member groups are placed in separate groups. This classification is useful especially to understand geological controls on water chemistry under conditions where useful geochemical data are available but clear hydrogeologic models have not yet been developed (Swanson et al., 2001). The advantage of HCA is that many variables such as physical, chemical or isotopic composition can be used to classify waters. In order that the variables have equal weight the raw chemical data should first be log-transformed and standardized. This restricts the influence of or the biases caused by the variables that have the greatest or the smallest variances or magnitudes on the clustering results. A detailed description of the advantages and uses of the HCA in hydrogeochemistry and the mathematical formulation behind HCA is thoroughly discussed in Swanson et al. (2001) and in Güler et al. (2002).

The ability of HCA to classify groundwater chemistry into coherent groups that may be distinguished in

terms of aquifer type, subsurface residence time and degree of human impact on water chemistry provides a good opportunity to conduct hydrogeochemical modeling and understand groundwater geochemical evolution among the different groups or subgroups. In this study, HCA is used to classify waters into objective groups and to conduct geochemical modeling among the different facies. A Microsoft *EXCEL* add-in module *XLSTAT4.3* was used to conduct the HCA.

3.3. Inverse geochemical modeling

Inverse geochemical modeling has been widely conducted in groundwater chemical evolution studies (Plummer et al., 1983; Kenoyer and Bowser, 1992; Varsanyi and Kovacs, 1997; Hidalgo and Cruz-Sanjulian, 2001; Wang et al., 2001). It is a useful approach to determine the type and amount in moles of minerals that dissolve or precipitate along a groundwater flow path. In the cases where information is available on the hydrogeology of the basin, the flow paths can be selected based on the hydrogeological knowledge. The initial and the final member can be chosen by taking into account the location of the point, the hydraulic heads of the aquifer system and observed trends in chemical evolution of the water (Kenoyer and Bowser, 1992; Varsanyi and Kovacs, 1997; Hidalgo and Cruz-Sanjulian, 2001). In areas where information on groundwater flow direction is lacking, the initial and final waters can be selected from the HCA groups. This is based on the logical assumption that waters which fall in a statistical group may have similar residence time, similar recharge history, and identical flow paths or reservoir (Swanson et al., 2001; Güler and Thyne, 2004). The PHREEQC computer code (Parkhurst and Appelo, 1999) was used to simulate the geochemical evolution among the average composition of statistical clusters.

4. Results and discussion

4.1. Chemistry and isotopic compositions of the waters and their spatial variation

Complementary geochemical and isotope hydrological data show that in general there are two types of groundwater systems in the upper Blue Nile basin. These are the low salinity, *Ca–Mg–HCO₃* type, isotopically relatively enriched cold (13–25 °C) groundwaters from the basaltic plateau and the high TDS, *Na–HCO₃* type, isotopically relatively depleted low temperature (25–40 °C) thermal groundwater systems from the deeply faulted grabens.

The majority of the groundwaters from the basaltic plateau are characterized by low TDS (generally less than 500 mg/L). Calcium and Mg dominate the cation species. They are characterized by *Ca–Mg–HCO₃* type water in the Piper plot (Fig. 3). In the general groundwater chemical evolution model (Plummer et al., 1990; Adams et al., 2001; Edmunds and Smedley, 2000), these types of waters are often regarded as recharge area waters which are at their early stage of geochemical evolution. Rapidly circulating groundwaters which have not undergone a pronounced water–rock interaction may also have similar characteristics.

The majority of the low temperature thermal groundwater springs from the YTVL and the LTG have high TDS (generally greater than 1000 mg/L). Sodium and K^+ dominate their cation species and HCO_3^- is the dominant anion. These groundwaters fall in the *Na–HCO₃* type groundwaters in the Piper plot. This is because with further hydrolysis of silicate minerals by the *Ca–Mg–HCO₃* type waters, the concentration of Na, K, Mg and HCO_3 increase but Ca enrichment is limited by an earlier saturation and precipitation of carbonates. The high TDS and the enrichment of sodium therefore testify that the thermal and the high TDS groundwaters have undergone a relatively pronounced degree of groundwater chemical evolution. High pH values are more often observed in the groundwaters of the basaltic plateau than in the high TDS *Na–HCO₃* groundwaters of the YTVL and LTG.

High F^- is observed in few water points issuing from acid volcanic rocks of the Quaternary acid volcanics in YTVL and in the groundwaters associated with thermal systems (e.g., samples SK2, SK3, SK4, SK80, SK93, and SK102). The high F^- in the groundwaters associated with acid volcanism has its source from leaching of F^- bearing accessory minerals. Fluoride from leaching of acid volcanic rocks is a widely accepted explanation of high F^- in the East African Rift Valley groundwaters (Darling et al., 1996; Gizaw, 1996; Chernet et al., 2001). Some rock forming minerals of acid volcanic rocks such as alkali amphiboles, alkali mica or accessory minerals such as apatite often contain F^- replacing OH^- groups in the minerals (Kilham and Hecky, 1973).

Shallow unprotected springs and unprotected wells contain high NO_3^- and Cl^-. The source of high NO_3 in groundwater of the region is often attributed to anthropogenic activity (agricultural or domestic waste) exacerbated by lack of well head or spring protection (McKenzie et al., 2001; Reimann et al., 2003).

Despite the high altitude (mean altitude ~2500 masl), the low mean annual air temperature (~17 °C) in the basin, and the furthest distance of Ethiopia from the Atlantic moisture source, the cold groundwaters of the basin do not show commensurate $\delta^{18}O$ depletion compared to modern meteoric waters of Sahelian Africa. This confirms the previous observation made from the isotopic composition of East African rainfall (Rozanski et al., 1996) and from the few groundwater isotope data across Sahelian Africa (Joseph et al., 1992).

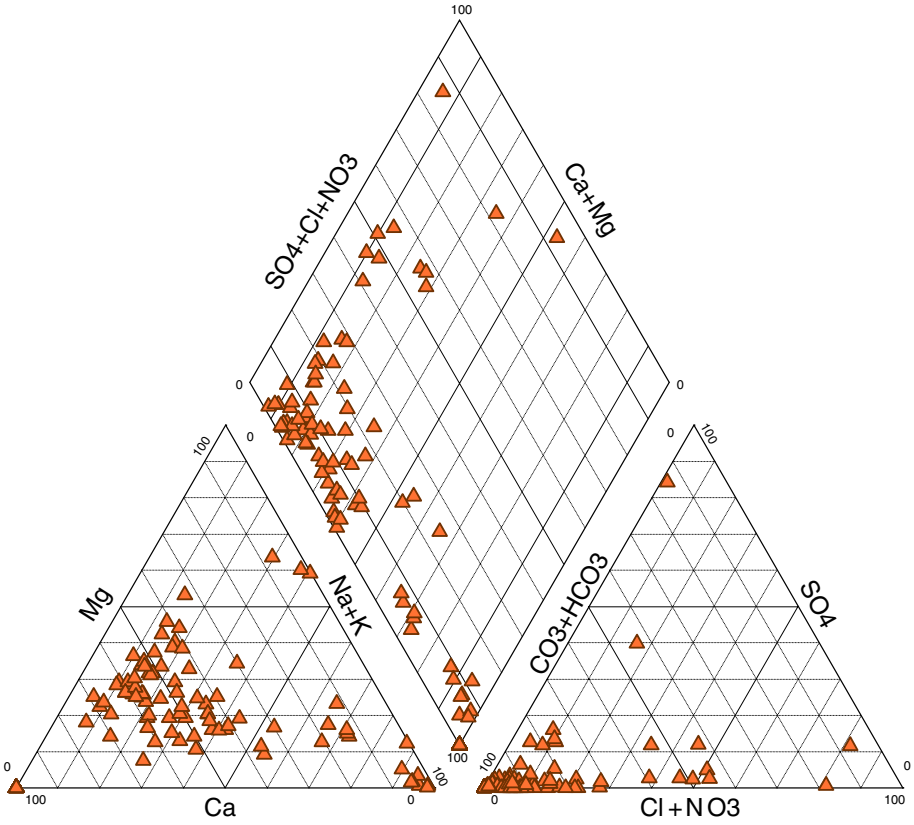

Fig. 3. Piper plot of the chemical data.

Unlike the Ethiopian Rift groundwaters and the groundwaters of shallow systems of the Sahel region, the groundwaters of the Blue Nile basin are characterised by high (>15) D excess. All the groundwaters plot above the Global Meteoric Water Line (GLWL) in a $\delta^{18}O$ vs. δD plot (Fig. 4). Lakes and rivers draining the lakes are enriched and they plots below the GMWL following a slope of 5.4. The Blue Nile River sampled at Khartoum (Farah et al., 2000) shows similar $\delta^{18}O$ and δD compositions to the groundwaters of the Blue Nile basin. This reflects both a rapid water transfer time from the Northwestern Ethiopian Plateau to the Sudan and lack of strong en route evaporative effects. A clear difference exists between the $\delta^{18}O$ and δD compositions of surface water originating from the Equatorial lakes region and the $\delta^{18}O$ and δD compositions of meteoric waters of the Blue Nile River. The former shows isotopic enrichment and plots below the GMWL owing to evaporation in the equatorial lakes. This distinct signal has been used as a basis for groundwater tracing (Farah et al., 2000) in Central Sudan where the two hydrologic systems merge. The low temperature thermal waters (hypothermal waters) and the high TDS *Na–HCO$_3$* type waters of the LTG and the YTVL are characterized by relatively highly depleted $\delta^{18}O$ compositions (Figs. 4 and 5). A tendency of depletion ($-0.1‰$/100 m) of $\delta^{18}O$ with altitude is observed in the low TDS cold groundwaters (Fig. 5). In general, the low TDS cold groundwaters in mountainous regions east and northeast of the Blue Nile basin are characterized by relatively depleted $\delta^{18}O$.

The $\delta^{18}O$ and δD compositions of the groundwaters are distributed around the average summer $\delta^{18}O$ and δD composition of Ethiopian rainfall. The average $\delta^{18}O$ of Ethiopian summer rainfall is $-2.5‰$ (Kebede et al., 2003). Some previous works (Gizaw, 2002) indicate the presence of dissimilarity and imbalance between groundwater and the annual average rainwater $\delta^{18}O$ and δD compositions. In the Blue Nile basin the groundwaters $\delta^{18}O$ and δD composition very well represents the average isotopic composition of Ethiopian summer rainfall as recorded at the Addis Ababa IAEA station. Lack of influence of evaporative concentration of the isotopes in groundwaters and the similarity between the isotopic compositions of the groundwaters and that of the composition of summer rainfall indicate that recharge occurs principally from summer rainfall. This rules out the importance of evaporative fractionation prior to re-

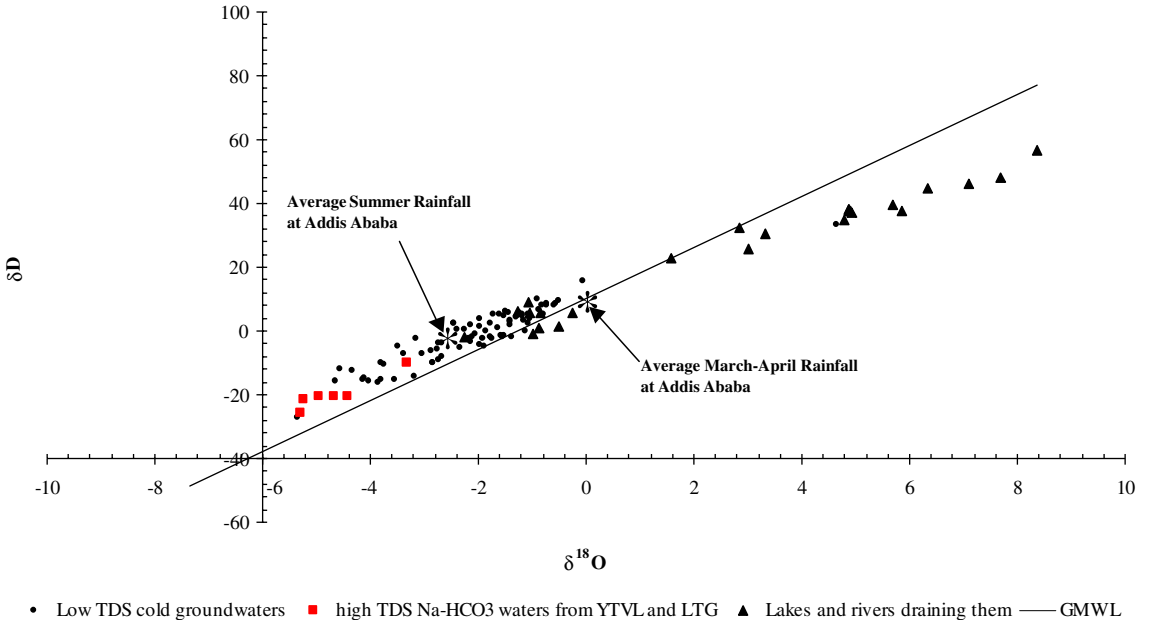

Fig. 4. Isotope plot of the water samples compared to the global meteoric water line (GMWL). The waters which plot below the GMWL are mostly lake waters from the basin.

charge in affecting the isotope signals. The spring rainfall O isotopic signature having $\delta^{18}O > 0‰$ (Kebede et al., 2003) is not commonly observed in the groundwaters. This testifies to the recharge to groundwaters taking place only from the summer rainfall ruling out the importance of the spring rainfall as a source of recharge.

Representative samples collected from the low TDS groundwaters from the basaltic plateau have appreciable concentrations of ^{3}H: SK46 (5.8TU), SK47 (3.6TU), SK48 (5.8TU), SK52 (3.8TU) and SK92 (6.8TU). The thermal and the high TDS groundwaters from the YTVL and the LTG contain low ^{3}H concentrations: SK80 (0.7TU), SK93 (0.5TU), and SK102 (0.5TU). This reflects deeper circulation of groundwater and older ages of the high TDS *Na–HCO₃* groundwaters.

The highly depleted $\delta^{18}O$ composition of the high TDS *Na–HCO₃* springs of the YTVL and the LTG (Figs. 4 and 5) indicate that recharge must have taken place at higher altitude sources. However the $\delta^{18}O$ of present day highest altitude cold springs are not as depleted as the $\delta^{18}O$ of the high TDS waters (Fig. 5). This indicates that recharge of the high TDS waters probably took place under a colder climate regime than today. The absence of an appreciable amount of ^{3}H in high TDS waters also testifies to a lack of any modern day meteoric water mixing with them. These waters must have followed deeper circulation pathways before they emerged as low temperature thermal waters.

Recharge to the high TDS waters of the LTG most likely takes place around the Guna and Debretabor Shield volcanoes (north of the Blue Nile basin). The Choke shield volcano in the center of the Blue Nile basin is the principal site of recharge to the Bure (SK15) high TDS springs. The Wolliso (SK80) and the Ambo (SK102) high TDS thermal springs are most likely recharged around the highland midway between the two regions.

The Wanzaye alkaline thermal springs (SK19) show specific isotopic and chemical characteristics. These springs are characterized by the most depleted $\delta^{18}O$ and δD isotopic compositions but they are also the most dilute with TDS less than 200 mg/L. The depletion in the isotopic composition reflects the presence of groundwater which has been recharged under colder climatic conditions in the Miocene lacustrine deposits.

Groundwaters in the Ethiopian Rift Valley east of the Blue Nile basin just out side the basin (Fig. 5) are relatively enriched in $\delta^{18}O$ compared to the groundwaters of the bordering highland. This indicates a lack of a strong subsurface link between the plateau in the eastern part of the Blue Nile basin and the shallow Rift Valley aquifers. The relative enrichment of the Rift Valley waters is related to the importance of evaporative fractionation before recharge (Kebede et al., 2003).

An important water body which may play a role as a recharge source for aquifers in the LTG is Lake Tana. But its influence on the nearby groundwater is not evident from the isotope plots. Groundwaters collected from around the southern, eastern and northern parts of the lake do not show any sign of enrichment caused

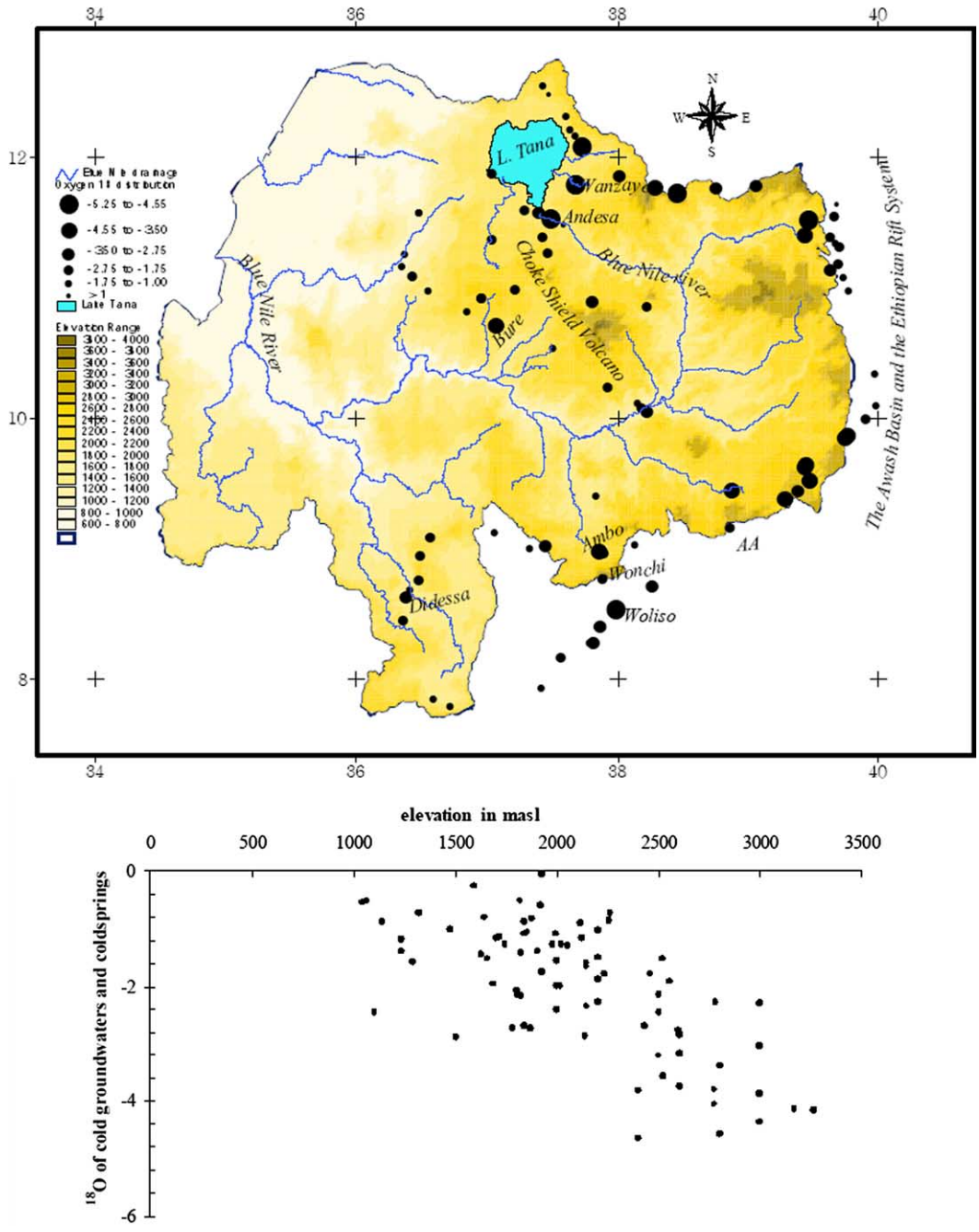

Fig. 5. Spatial and altitudinal variation of $\delta^{18}O$ in groundwaters of the basin. The size of the symbols reflects the degree of depletion in $\delta^{18}O$. The average depletion of $\delta^{18}O$ vs. altitude is $-0.1‰/100$ m. The most depleted waters around lake Tana (Andesa and Wanzaye) and in the YTVL (Ambo, Woliso, Wonchi and Dedesa) are the high TDS low temperature thermal spring.

by mixing of lake water into them. This lack of groundwater outflow from the lake is the result of the lake-ward dipping blocks of rocks that favor groundwater flow to the lake rather than loss of lake water into the surrounding aquifers.

4.2. Statistical clusters and their correlation with hydrogeology

Statistical classification of the hydrochemical data is used here to elaborate the fore going water geochemical

types and associated chemical processes. Eleven variables (pH, Ca^{2+}, Mg^{2+}, K^+, Na^+, HCO_3^-, CO_3^{2-}, Cl^-, SO_4^{2-}, TDS) were considered to classify the 86 groundwater samples with complete chemical analysis (Appendix 1, see web version). In HCA the variables are log transformed and normalized so that each variable will have equal weight. Groups were selected visually from the dendrogram (Fig. 6) which is the output of the clustering. From the dendrogram, 2 major groups and 9 subgroups were chosen using an index of similarity = 0.25. This index of similarity was chosen because the 9 sub groups of waters that result were very clearly distinguishable in terms of their hydrogeological and geological variables. The two major groups are distinguished by their TDS. Group I (deep systems) waters have TDS greater than 1200 mg/L. Group II (shallow systems) waters have TDS less than 800 mg/L. The two groups also have distinct $\delta^{18}O$, δD, ^3H and $\delta^{13}C$ compositions. Group I waters are depleted in $\delta^{18}O$ and δD, they are almost ^3H free, and they are enriched in $\delta^{13}C$. Group II waters are generally enriched in $\delta^{18}O$ and δD, they contain appreciable amount of ^3H and have depleted $\delta^{13}C$. Group I waters have 5 subgroups and Group II waters have 4 subgroups. Group I contains 5 fairly distinguishable subgroups. Group II have 3 distinguishable subgroups.

The samples grouped under each subgroup and the average physico-chemical composition of each subgroup are presented in Table 1 and Fig. 7. There is a good statistical coherence among the average subgroups, that is, the chemical composition of the subgroups can be clearly explained in terms of geologic history, aquifer type, and the human impact on water quality. Correlation of the average composition of the subgroups and the accompanying geological features is given in Table 2. The ability of the statistical analysis to classify the groundwaters into these distinct categories of geological context helped the authors to gain additional insight on groundwater flow patterns and to conduct inverse geochemical modeling on the subgroups.

The HCA also shows that groundwaters which plot near each other in a simple Piper plot (Figs. 3 and 7) may not be necessarily similar in their chemical evolution history. Waters of subgroups II, III, VII and VIII which plot near each other in the Piper plot are statistically and geologically distinct. The same is true for waters of subgroups IV, V and VI.

The concentration of Ca^{2+} decreases generally from the more dilute groups to the high TDS groups (except in subgroup I). This may reflect precipitation of calcite along the flow path when the groundwater is transferred from the shallow to the deeper systems. Many of the ions (K^+, Na^+, Mg^{2+}, HCO_3^-, F^-, Cl^-, SiO_2) increase from the dilute systems to the high TDS systems. Exceptions to these are subgroup I and subgroup VI. The general increase in Mg^{2+}, Na^+, K^+, SiO_2 reflect the increased amount of hydrolysis of silicate minerals such as olivines, pyroxenes, plagioclase and alkali feldspars. The pH generally decreases from the shallow to the deeper systems testifying additional input of CO_2 gas. The concentration of NO_3^- is generally higher in the shallow systems than in the deep systems indicating a recent increase in pollution of the shallow groundwaters. Generally high TDS groundwaters from the YTVL contain the highest F^- contents. All the water groups are saturated or supersaturated with respect to silica. This reflects a relatively rapid hydrolysis of ferromagnesian minerals of the basaltic aquifers. The silica content however is higher in the high TDS systems because the high temperature of these groundwater systems increases the solubility of silica.

All the waters subgroups except subgroup I are undersaturated with respect to gypsum and anhydrite testifying that these minerals which abundantly exist in the sedimentary layers are not the main limiting factors of the concentrations of SO_4^{2-}. Only one cold spring sample (SK9) which emerges from the Mesozoic sedimentary layers is near saturation with respect to gypsum and anhydrite. The high TDS *Na–HCO₃* low temperature thermal springs are undersaturated with respect to the carbonate minerals (calcite, aragonite and dolomite), though deposition of these minerals are common around the springs. This may testify that disequilibrium (undersaturation) in these waters is caused by external input of CO_2 gas from deeper sources which joins the groundwaters at shallower depths. Under this condition the groundwaters may not have enough time to dissolve more carbonate minerals to reach equilibrium conditions.

The statistical classification also shows that at least two geochemical types of groundwater exist in the basaltic plateau. Waters of subgroup IX generally represent shallow circulation while those in sub group VII represent deeper circulation in the basaltic plateau. The concentration of all the major elements (except SiO_2 and Ca^{2+}) the pH and the TDS increase from subgroup IX to subgroup VII. The waters of subgroup VII are saturated with respect to silica and calcite while waters of subgroup IX are under saturated with respect to these minerals. These compositional differences imply the presence of at least two groundwater layers in the basaltic aquifers. Hydrolysis of volcanic minerals leads to increase in pH and the increase in the concentration of major elements when the water is transferred from the shallow basaltic aquifers to the deeper basaltic aquifers. Subgroup VIII represents polluted members of the shallow groundwaters from the basaltic plateau.

4.3. Geochemical modeling and groundwater chemical evolution

Inverse geochemical modeling was conducted on the water subgroups that resulted from HCA. The average

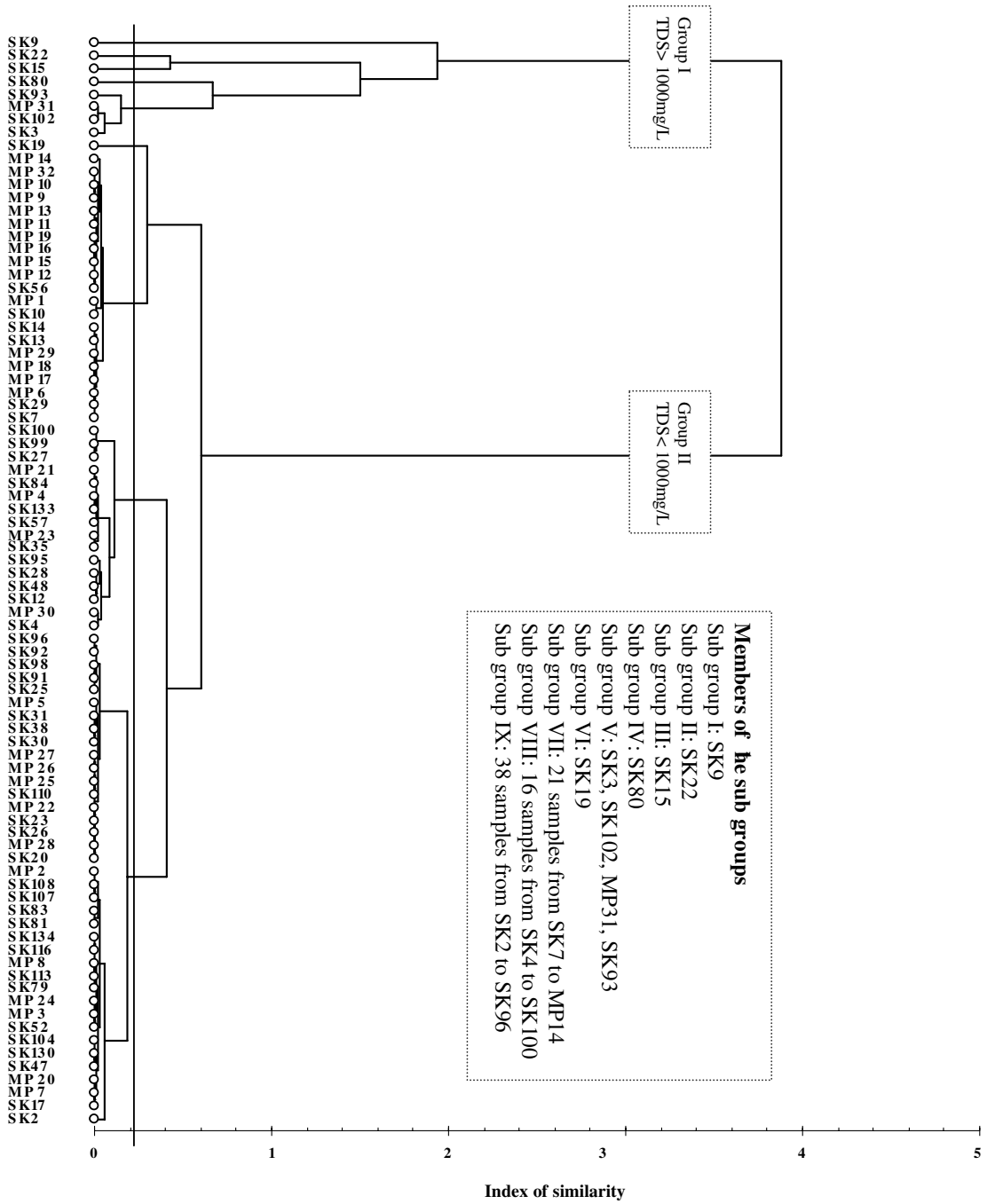

Fig. 6. Dendrogram of the Q-mode hierarchical cluster analysis. The 'phenon line' is chosen at similarity index = 0.25 to select 9 subgroups. The left most subgroup is subgroup I and the right most ones are subgroup IX. The samples which belong to each subgroup are listed under the branches and in the box in the upper corner.

chemical composition of waters of subgroup IX was assumed to represent a pristine recharge area groundwater. Its composition is therefore taken as 'initial' water in the inverse geochemical modeling. The remaining subgroups were considered to be derived from this subgroup. Two exceptions are waters of subgroup VI and I. Subgroup VI has lower TDS and high pH so that it is not possible for it to originate from the average of subgroup IX under the logical assumption that the final waters in the inverse modeling have higher TDS than the

Table 1
Mean values of chemistry of groundwater subgroups, numbers in the superscript indicate the number of members of the subgroup, ^3H and $\delta^{13}C$ concentrations are measured on selected representative samples of the subgroups

Subgroup	pH	TDS	K^+	Mg^{2+}	Na^+	Ca^{2+}	HCO_3	CO_3^{2-}	SO_4^{2-}	Cl^-	F^-	NO_3^-	SiO_2	P_{CO_2}	SI-C	SI-G	SI-Ch	^3H	$\delta^{13}C$ (‰)
I^1	*7.67*	*3514*	*7.2*	*149*	*62.2*	*670.8*	*442.9*	*4.1*	*2142*	*25.6*	*1.25*	*9.2*	*23.7*	0.008	+1.42	+0.35	+0.15		
II^1	*8.11*	*3922*	*14.8*	*336*	*426*	*1.2*	*3081*	*50*	*5.1*	*8.0*	*0.06*	*0.04*	*113*	0.021	0.00	−4.92	+0.82		*+1.0*
III^1	*6.53*	*4596*	*28.3*	*462*	*531*	*22.9*	*3500*	*1.8*	*18.4*	*30.2*	*0.06*	*1.5*	*124*	0.900	−0.27	−3.13	+0.88		*+4.8*
IV^1	*7.75*	*1099*	*11.9*	*20*	*262*	*1.6*	*732*	*2.7*	*0.1*	*39.2*	*26.6*	*2.3*	*119*	0.013	−0.67	−6.20	+0.85	*0.7*	*−4.5*
V^4	*6.78*	*1781*	*27.3*	*21.2*	*415*	*29.8*	*1209*	*0.6*	*27.2*	*36.8*	*3.1*	*11.3*	*128*	0.189	−0.20	−2.58	+0.88	*0.5*	*+1.5*
VI^1	*9.15*	*128*	*0.4*	*0.02*	*43.2*	*0.6*	*44*	*35*	*2.1*	*2.6*	*0.39*	*0.04*	*66.2*	<0.001	−0.76	−5.07	+0.51		*−15.5*
VII^{21}	*8.15*	*328*	*2.3*	*8.9*	*45*	*28.9*	*211.2*	*2.4*	*14.8*	*9.3*	*0.24*	*4.69*	*30.2*	0.002	+0.53	−2.63	+0.24		*−11.6*
$VIII^{16}$	*6.99*	*461*	*4.9*	*17.7*	*37.8*	*52.4*	*281.4*	*0.4*	*9.3*	*19.9*	*0.26*	*37.1*	*62.0*	0.029	−0.27	−2.62	+0.57		
IX^{38}	*6.88*	*191*	*2.0*	*7.9*	*10.4*	*25.2*	*135.7*	*0.1*	*1.3*	*3.1*	*0.30*	*5*	*55.6*	0.018	−0.97	−3.70	+0.52	*6.8*	

The saturation indices of calcite (SI-C) gypsum (SI-G) and chalcedony (SI-Ch) are also presented for the average group.

initial waters. Field evidence shows that waters of subgroup I get their recharge directly from rainfall without passing through chemical characteristics of waters of subgroup IX. Therefore the lowest TDS groundwater (SK92) was used as the initial water to simulate the composition of subgroups VI and I.

The mineral phases were selected based on the saturation indices and the general mineralogical compositions of the rocks in the basin. The result of the inverse geochemical modeling (Table 3) shows that, except in the evolution towards subgroup I, the hydrolysis of silicate minerals (principally feldspars and ferromagnesian minerals) without a major involvement of the sedimentary minerals (e.g., carbonates, evaporites) can satisfy the simulation. The major minerals that are required to dissolve were olivine, pyroxene, plagioclase, K–micas and K–feldspars. Dissolution of gaseous CO_2 is required in all cases. Removal of clay minerals such as illite or Ca–montmorillonite was required during groundwater transition in the aquifers. Precipitation of calcite or chalcedony or both were required in the models. Dissolution of gypsum, dissolution of dolomite and cation exchange ($CaX \leftrightarrow NaX$) were required to simulate the composition of subgroup I. While hydrolysis of olivines and pyroxenes were the principal reactions required to simulate group II and III waters, Plagioclase, K–feldspars and K–mica were the major phases required to simulate subgroups IV and V.

4.4. Further insight on groundwater chemical evolution: the role of CO_2

4.4.1. Geochemical evidence – carbonate species

One important observation that emerged from the carbonate species composition of the groundwaters and the HCA is the presence of 4 types of groundwater system as far as the role of CO_2 is concerned. This distinction is made based on the relation between pH, HCO_3^- and TDS (Fig. 8). The 4 systems represent different degrees of involvement of CO_2 in the chemical evolution. The 4 systems can also be distinguished based on their $\delta^{13}C$. The 4 systems are, (a) subgroups III and V: a very low pH, high HCO_3^- and high TDS thermal springs; (b) subgroup II and IV: a near neutral pH, high HCO_3^- and high TDS groundwaters; (c) subgroup VI: a very high pH low TDS and low HCO_3^-; and, (d) subgroup IX, VIII, VII, and I: near neutral pH, low HCO_3^- and variable TDS.

One important point about the chemistry of thermal groundwater springs of subgroups III and V is the presence of high partial pressure of CO_2 and high HCO_3^-. Partial pressure of CO_2 high as 0.9 atm (Table 1) and concentration as high as 4000 mg/L have been reported (BCEOM, 1999) in these springs. All the waters with these characteristics emerge as hot springs exclusively in the LTG and in the YTVL. The high partial pressure

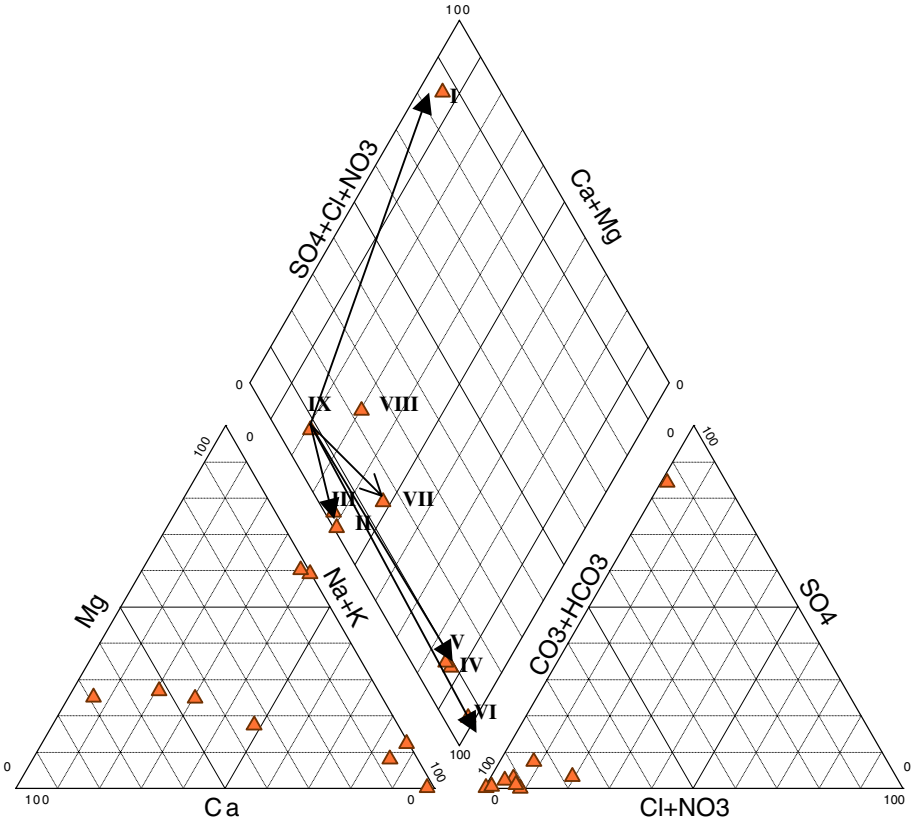

Fig. 7. Piper plot of the subgroups, groundwater which plot near each other in a Piper plot may not always be similar in their geochemical evolution history. The lines are some of the paths selected for the inverse geochemical modeling.

of CO_2 coupled with the high mineralization, the low pH, the relatively high temperature, and the fact that they emerge along the deep grabens and associated lineaments testify that the system is open to an external input of CO_2 from deeper sources. The relatively depleted $\delta^{18}O$ composition of these waters and the very low ^3H content reveals a recharge source at high altitude far from the emanation point of the springs. These in turn reflect a deep circulation of groundwater and long subsurface residence time. The source of CO_2 may be a direct source from the mantle along the deep faults or from metamorphic decarbonation of the underlying sedimentary sequence by heat from a magma chamber – the same magma chamber which has led to the eruption of the Quaternary volcanoes in the YTVL and the formation of Quaternary basalts in the LTG.

Two exceptions of the high TDS *Na–HCO₃* waters that may not be completely explained by the above model are the Bure cold springs (subgroup II) and the Wolliso thermal springs (subgroup IV). These two waters evolve with lower amounts of CO_2 involvement compared to subgroup III and V waters. While lack of heating from below restricts the decarbonation and major influx of CO_2 from the Mesozoic sediments in the Bure cold spring area, lack of or the thinning of the Mesozoic formation in the southern part of the YTVL restricts major influx of CO_2 from deeper sources.

Waters of subgroup VI shows unique characteristics. They have very high pH, extremely low P_{CO_2} and very low TDS. They are associated with a faulted area in the eastern part of the LTG. The isotopic signature of these waters indicates that they have meteoric origin. Their depleted $\delta^{18}O$ relative to nearby groundwater bodies may indicate that recharge takes place at high altitude. Unlike the other thermal springs in the Blue Nile basin, this water contains an extremely low amount of dissolved CO_2. Sodium, HCO_3^- and SiO_2 dominate the chemistry. Calcium and Mg^{2+} are extremely low. One of the most plausible explanations for the existence of these hyperalkaline, very low TDS thermal springs is that these waters interact with a metamorphosed Miocene lacustrine lignite and mud rock beds imbedded between the trap series basalts. This metamorphosed zone could act as major sink zone for CO_2, Ca^{2+} and Mg^{2+} with an increase in Na^+, K^+, pH, and SiO_2 leading to this unique characteristic. These kinds of hyperalkaline

Table 2
Description of the geologic characteristics accompanying the statistical subgroups

Cluster	Geology
Subgroup I[1]	The only cold spring from Mesozoic succession of the Blue Nile gorge. This spring emerges at a contact between evaporite beds and a thick sequence of limestone
Subgroup II[1]	A high TDS slightly alkaline pH cold spring from the Bure fault zone in the Ethiopian Plateau, no indication of thermal activity is observed in the region, the spring emerges at a contact between the Cenozoic trap basalt and the underlying Mesozoic sandstone. These springs have depleted $\delta^{18}O$
Subgroup III[1]	A high TDS, very low pH, thermal/cold spring from the LTG. Travertine deposits were observed at the issuing point of these springs. These springs have depleted $\delta^{18}O$
Subgroup IV[1]	A near neutral pH, high TDS thermal spring in the southern part of YTVL. Underneath the area where these springs emerge the Mesozoic strata is very thin or absent. This spring is similar to sub group V waters but it contains lower P_{CO_2}
Subgroup V[4]	A low pH group of thermal springs in a deeply faulted region of the YTVL, these subgroups are distinct from subgroup III water by their Mg content. While basalts are the dominant rock outcrop around subgroup III waters, quaternary acid volcanic rocks dominate the recharge region of subgroup V waters. Thick travertine and silica sinter deposits are ubiquitous around the issuing point of these springs
Subgroup VI[1]	A hyperalkaline, very low TDS thermal spring east of the LTG. The geology of the area where this spring emerges is distinct by the presence of beds of late Miocene lignite, organic marls and Pliocene lacustrine deposits. There are 3 springs of this nature within a radius of 5 km
Subgroup VII[21]	Low TDS, relatively high pH springs and groundwaters from the basaltic plateau. The majority of these waters are deep wells from the basaltic plateau. These waters are saturated with respect to calcite. The relatively high pH and HCO_3 and the saturation indices shows that these subgroups are derived from the subgroup IX waters by silicate hydrolysis
Subgroup VIII[16]	Low TDS, relatively high pH, high NO_3 and high Cl cold springs and groundwater wells from basaltic plateau. These waters are affected by pollution because of lack of well-head or spring protection
Subgroup IX[38]	Very low TDS, low pH, Ca–HCO_3 type cold springs and shallow wells which may represent geochemically unevolved young meteoric waters from the basaltic plateau. These waters are mainly collected from hand-dug wells and cold springs. These waters are under saturated with respect to calcite, aragonite and gypsum. Some members of this group contains appreciable amount of ^3H testifying shallow circulation

very low TDS waters are not uncommon. Clark et al. (1994) have reported the presence of a similar type of thermal springs in an area characterized by a similar geologic condition (high heat flow and covered by metamorphosed organoclastic deposits).

The remaining subgroups (subgroup VII, VIII, IX, I) evolve under relatively closed system silicate hydrolysis and dissolution reactions. Under such conditions, the initial H^+ produced by the reaction between soil CO_2 and the infiltrating water will be consumed by the silicate hydrolysis reaction. Because of lack of additional CO_2 from deeper sources both the pH and HCO_3^- increase along the evolution direction SK92 → IX → VII or along SK92 → I until saturation is reached with respect to carbonate minerals. The relatively deeper systems of the basaltic plateau (subgroup VII) are more closed to external input of CO_2 than the shallower systems of the basaltic plateau (subgroup IX).

4.4.2. Carbon-13 evidence

Carbon-13 were measured in 6 samples each one representative of different groundwater subgroups. The $\delta^{13}C$ content of the high TDS *Na–HCO₃* groundwaters varies between −4.2‰ and +6.3‰ PDB. These compositions are more enriched than the $\delta^{13}C$ compositions of mantle CO_2 which varies between −3‰ and −8‰ (Hoefs, 1997). This enriched range of $\delta^{13}C$ is most likely the result of interaction of groundwaters with CO_2 from metamorphic decarbonation of carbonate rocks beneath

Table 3
Summary of inverse modelling for selected paths

Path	Reaction
SK92-Subgroup I	**Gypsum** + **Dolomite** + Halite + NaX from ion exchange + CO_2 (g) → Ca–SO_4 water + Ca loss to ion exchange + **Chalcedony**
IX-Subgroup II	**Plagioclase** + **Olivene** + **Pyroxene** + K–mica + CO6 (g) → Na–Mg–HCO_3 water + **Illite** + **Calcite** + Fluorite
IX-Subgroup III	**Plagioclase** + **Olivine** + **Pyroxene** + K–mica + trace gypsum + CO_2 (g) → Na–Mg–HCO_3 water + **Calcite** + **Illite** + trace fluorite
IX-Subgroup IV	**Plagioclase** + **Pyroxene** + **K–mica** + trace fluorite + CO_2 (g) → Na–HCO_3 water + **Chalcedony** + Ca montmorilonite + trace Gypsum
IX-Subgroup V	**Plagioclase** + Pyroxene + **K–feldespar** + trace gypsum and fluorite → Na–HCO_3 water + **Chalcedony** + **Calcite** + **Illite**
IX-Subgroup VII	**Plagioclase** + **Pyroxene** + **K–mica** + trace gypsum + CO_2(g) → Ca–Mg–HCO_3 water + **Illite**

The majority of the phases and thermodynamic data are taken from PHREEQC database (Parkhurst and Appelo, 1999) and from Kenoyer and Bowser (1992).

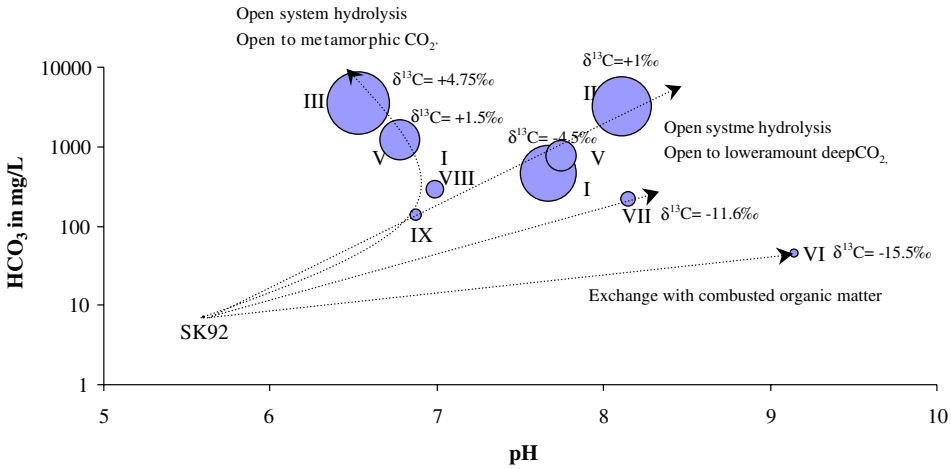

Fig. 8. pH vs. HCO_3 plot to show the role of external input of CO_2 in chemical evolution of groundwaters, size of the circles reflects the TDS. Some $\delta^{13}C$ are also given.

the YVTL and the LTG. This is the most plausible mechanism because the $\delta^{13}C$ of CO_2 of carbonate rocks ranges between −4% and +4% (Craig, 1963). This confirms the geochemical evidence from pH, HCO_3 and TDS of the influence of deep CO_2 from deeper metamorphic decarbonation sources on the high TDS waters. Waters of subgroup III and V are relatively more depleted in $\delta^{13}C$ than waters of subgroup II and IV confirming the hypotheses from the carbonate species compositions that relatively lower amount of deep CO_2 is involved in the geochemistry of these springs.

The Jiga cold springs (SK103) representative of the shallow *Ca–Mg–HCO₃* type groundwaters show a $\delta^{13}C$ of −11.6‰ reflecting soil CO_2 as a principal source of carbonate species in the shallow groundwaters. Cold groundwaters from basaltic aquifers around Addis Ababa (on the southern water divide of the Blue Nile Basin) show a $\delta^{13}C$ ranging between −4‰ and −12‰ (Gizaw, 2002). These testify to the dominant source of CO_2 in the shallow groundwaters of the basaltic plateau being soil CO_2.

The Wanzaye thermal springs (subgroup VI) are the most depleted in both $\delta^{13}C$ ($\delta^{13}C = -15.5‰$) and $\delta^{18}O$ (−5.4‰) contents. The very high pH of these springs, the extremely low P_{CO_2}, its *Na–HCO₃* nature, and the depletion in $\delta^{18}O$ shows that these springs represent evolved groundwater systems which have undergone a significant degree of water–rock interaction. The extreme depletion of $\delta^{13}C$ of these springs confirms the hypothesis from geochemical evidence that they must have interacted with organic matter at depth. These reflect that the Wonzye thermal springs interact with organic matter of the Miocene organic rich sediments in the LTG.

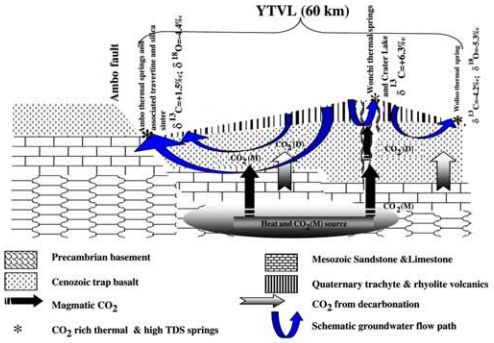

1. Recharge at high altitude by *Ca-HCO$_3$* type waters, major residence in acid volcanic rocks, open system hydrolysis of silicate minerals, lowering of pH by addition of CO_2 from metamorphic decarbonation of the underlying Mesozoic sediments or from direct CO_2 input form deeper sources along the fault zone, release of CO_2 on emergence or before emergence and deposition of travertine and silica sinter, waters with *Na-HCO$_3$* characteristics as final composition.

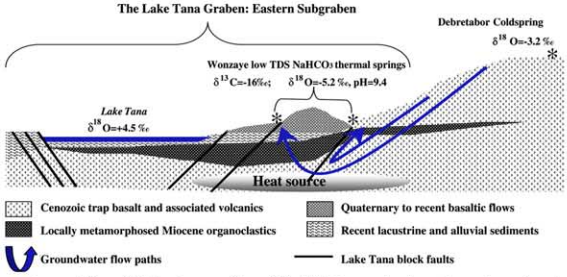

2. Recharge at around Guna Shield volcanoes, flow of *Ca-HCO$_3$* type water through a metamorphosed zone of the Miocene lignite beds and sink of CO_2, exchange of Ca for Na and K in the zone, formation of high pH and high SiO_2 water plume, emergence of *Na-HCO$_3$* water plume at low TDS and high pH.

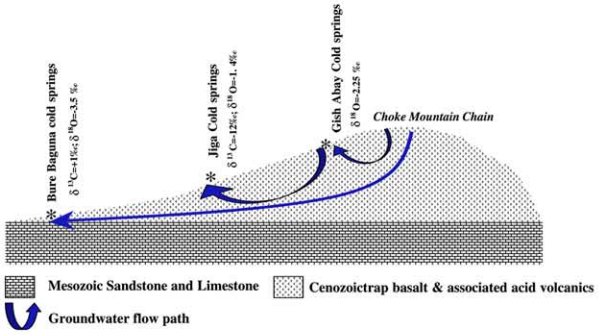

3. Recharge at high altitude around shield volcanoes of the central part of the Blue Nile basin, major subsurface residence of the water in the basaltic aquifer, closed system dissolution of silicate minerals without major addition of CO_2 from depth, emergence of the water at a contact between the Mesozoic and the Cenozoic as *Na-Mg-HCO$_3$* water at above neutral pH.

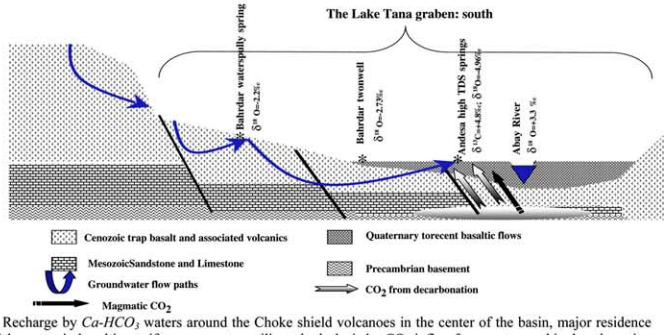

4. Recharge by *Ca-HCO$_3$* waters around the Choke shield volcanoes in the center of the basin, major residence of the water in basaltic aquifer, open system silicate hydrolysis by CO_2 influx from metamorphic decarbonation of the Mesozoic sediments or from a direct input of CO_2, deposition of travertine and silica sinter upon emergence, and formation of low pH, *Na-Mg-HCO$_3$* waters.

Fig. 9. Schematic sections showing origin and evolution of selected groundwater systems/springs. 1 – Thermal springs in the YTVL, 2 – Wonzaye thermal springs in LTG, 3 – Bure cold springs on the plateau, 4 – Andesa thermal spring in LTG.

5. Summary and conclusions

The Hierarchical Classification Analysis elaborately classified the groundwaters of the upper Blue Nile basin into two major groups and 9 subgroups. The advantage of the method was that the subgroups were objective and a clear geo-hydrological patterns were recognized. The 9 subgroups show different degrees of water–rock interaction, subsurface residence time, aquifer composition, influence of CO_2, and exposure to pollution, etc. In a poorly known hydrogeological system the exercise of associating the results of the cluster with geo-hydrological conditions facilitates the understanding of the groundwater flow systems in the basin. Traditionally, it was thought that two groundwater layers (shallow/deep; fresh/saline, unconfined/confined) exist in volcanic aquifers of the region (Chernet, 1982, 1990). However, the Hierarchical Classification Analysis and the geochemical approach show that more groundwater flow patterns can be distinguished in the region adding more understanding to the previous knowledge of the Ethiopian plateau volcanic hydrogeology.

The geochemical, isotopic, stratigraphic and structural data, and the Hierarchical Classification Analysis helped to schematize geo-hydrological characteristics of important zones in the Blue Nile basin and to gain for the first time a general picture of the groundwater circulation and its chemical evolution in the basin. Conceptual models that schematize the major geochemical processes and recharge source for selected groundwater systems are presented in Fig. 9.

In the basaltic plateau recharge is rapid, groundwater circulation is shallow and the waters are characterized by low TDS. Two structurally deformed zones, namely the LTG and the YTVL plays a major role in favoring the existence of regional and probably deeper groundwater flows. The geologic processes which formed the two structural basins resulted in juxtaposition of the Mesozoic sediments with the Cenozoic volcanic cover and this promotes the presence of artesian springs at the contact between the Mesozoic sediment and Cenozoic volcanic cover. Furthermore CO_2 from deeper sources (CO_2 produced by metamorphic decarbonation of the Mesozoic sediments underlying the basaltic trap) along the deformed zones influences geochemical evolution of the high TDS thermal groundwaters of the YTVL and the LTG. The CO_2 gas from depth promotes acid hydrolysis of the volcanic cover, which explains the generally low pH and high HCO_3^- of these groundwaters.

Despite the similarity in climatic conditions and the general similarity in Mesozoic lithology, the hydrogeological characteristics of the Blue Nile basin are different from the Hydrogeology of Sahelian Africa. The majority of groundwaters of the Blue Nile basin are often highly flushed, young, low TDS groundwaters with rapid recharge through fractured rocks. These characteristics are mainly the result of uplifting and erosional fragmentation of the aquifers of the Blue Nile basin. In the shallow sedimentary aquifers of the Sahel, evaporation prior to recharge seems an important hydrologic process (Sonnntag et al., 1982; Dodo and Zuppi, 1997). This process seems unimportant in the upper Blue Nile basin. The classical sedimentary basin aquifer (Intercalaire aquifers) that underlies the majority of the Sahel and Northern African countries (Sudan, Chad, Senegal, Mali, Niger, Tunisia, Egypt, etc.) containing late Pleistocene or early Holocene groundwaters (Sonnntag et al., 1982; Andrews et al., 1994; Edmunds et al., 2003; Dabous and Osmond, 2001) is represented by uplifted Mesozoic sediments which are not accessible to groundwater circulation due to the thick (often greater than 1 km) basaltic cover. In some places such as the LTG and the YTVL, however, the Mesozoic sediments play an indirect role in influencing the hydrogeochemistry of the groundwaters by supplying CO_2 for water–rock interaction.

The important role that CO_2 from deeper sources plays in groundwater chemical evolution is a widely accepted model in the East African Rift System also. In general, the $\delta^{13}C$ content of the high TDS groundwaters of the Blue Nile basin is more enriched than the $\delta^{13}C$ content of groundwaters of the Ethiopian Rift Valley, the $\delta^{13}C$ of the latter as documented in Darling et al. (1996) and Craig et al. (1977). This reflects that CO_2 from decarbonation of marine carbonates is more important in the Blue Nile basin high TDS thermal groundwaters than in the Rift Valley groundwaters. Many previous models (Darling et al., 1996; Gizaw, 2002) consider the source of CO_2 in thermal groundwaters of the Central Ethiopian Rift or that of the Addis Ababa region is the mantle and the influence of Metamorphic CO_2 is non existent or minor. Structural evidence coupled by geochemical data shows that the YTVL is an extensive east–west zone that intersects the Ethiopian Rift Valley. The influence of the Mesozoic sedimentary layers as a source of CO_2 in thermal groundwaters may not be minor beneath Addis Ababa and the Main Ethiopian Rift Valley as was previously thought.

The information obtained and the major conclusions found in this study will help to select future targets of detailed groundwater resource assessment programs. The schematic diagrams may be used to select suitable sites for groundwater resource development. The recently flourishing Ethiopian *Gaseous Soda Spring* bottling plants may find the schematic diagrams and the water quality data very useful. The isotope and geochemical data from the Blue Nile basin also allowed the authors in an independent work (Kebede et al., 2003) to trace the subsurface hydrogeologic link between the Northwestern Ethiopian Plateau and the Ethiopian Rift Valley.

Acknowledgements

This research was funded partly by the French Ministry of Foreign Affairs through its office at the French Embassy in Ethiopia. The first author thank the Ethiopian American Foundation for financial support for travel within Ethiopia during the collection of water samples. The Department of Geology and Geophysics, Addis Ababa University provided field vehicle and other field logistics. This work would not have been completed without the isotope analysis provided by The International Atomic Energy Agency through its TC project (ETH/8/007). Thanks also to Drs. Dereje Ayalew, Tesfaye Korme and Balemwal Atnafu for their constructive comments and discussions during the start of this work. This paper is part of the first author's dissertation research. Last but not least we thank one anonymous reviewer, Prof. M. Edmunds and Prof. Yves Tardy for constructive comments which helped us bring this article to publishable quality.

Appendix A. Supplementary data

Supplementary data associated with this article can be found, in the online version, at doi:10.1016/j.apgeochem.2005.04.016.

References

Abate, B., Koberl, C., Buchanan, C.P., Korner, W., 1996. Petrography and geochemistry of basaltic and rhyodacitic rocks from Lake Tana and the Gimjabet-Kosober areas (North Central Ethiopia). J. Afr. Earth Sci. 26, 119–134.

Abebe, T., 2000. Geological limitations of a geothermal system in a continental Rift zone: example the Ethiopian Rift Valley. In: Proc. World Geothermal Congress 2000, Kyushu – Tohoku, Japan, May 28–June 10, 2000.

Abebe, T., Mazzarini, F., Innocenti, F., Manetti, P., 1998. The Yerer-Tullu Wellel volcanotectonic lineament:a transtensional structure in central Ethiopia and the associated magmatic activity. J. Afr. Earth Sci. 26, 135–150.

Adams, S., Tredoux, G., Harris, C., Titus, R., Pietersen, K., 2001. Hydrochemical characteristics of aquifers near Sutherland in the Western Karoo, South Africa. J. Hydrol. 24, 91–103.

Alberto, W.D., Del Pilar, D.M., Valeria, A.M., Fabiana, P.S., Cecilia, H.A., De Los Angeles, B.M., 2001. Pattern recognition techniques for the evaluation of spatial and temporal variations in water quality. A case study: Suquýà River Basin (Cońdoba – Argentina). Water Res. 35, 2881–2894.

Andrews, J.N., Fontes, J.-C.h., Aranyossy, J.-F., Dodo, A., Edmunds, W.M., Joseph, A., Travi, Y., 1994. The evolution of alkaline groundwaters in the Continental Intercalaire aquifer of the Irhazer Plain, Niger. Water Resour. Res. 30, 45–61.

Asrat, A., Barbey, P., Gleizes, G., 2001. The Precambrian geology of Ethiopia: a review. Afr. Geosci. Rev. 18, 271–288.

Assefa, G., 1991. Lithostratigraphy and Environment of deposition of the Late Jurassic–Early Cretaceous sequence of the central part of northwestern plateau, Ethiopia. Neues Jahrb. Geol. Paleontol. Abhandubglen 182, 255–284.

Ayenew, T., 1998. The hydrogeological system of the lake district basin, central Main Ethiopian Rift. Ph.D. Thesis, ITC Publication Number 64, The Netherlands.

Barbieri, P., Adami, G., Favretto, A., Lutman, A., Avoscan, W., Reisenhofer, E., 2001. Robust cluster analysis for detecting physico-chemical typologies of freshwater from wells of the plain of Friuli (northeastern Italy). Anal. Chim. Acta 440, 161–170.

BCEOM, 1999. Abay River Basin integrated master plan, main report, Ministry of Water Resources, Addis Ababa.

Chernet, T., 1982. Hydrogeology of the lakes region, Ethiopia. Ministry of Mines and Energy, Addis Ababa.

Chernet, T., 1990. Hydrogeology of Ethiopia and water resources development, Ministry of Mines and Energy report.

Chernet, T., Travi, Y., Valles, V., 2001. Mechanism of degradation of the quality of natural water in the lakes region of the Ethiopian Rift Valley. Water Res. 35, 2819–2832.

Chorowiz, J., Collet, B., Bonavia, F., Mohr, P., Parrot, J.-F., Korme, T., 1998. The Tana basin, Ethiopia. Intra-plateau uplift, rifting and subsidence. Tectonophys. 295, 351–367.

Clark, D.I., Dayal, R., Khoury, H.N., 1994. The Maqarin (Jordan) natural analogue for ^{14}C attenuation in cementitious barriers. Waste Manag. 14, 467–477.

Craig, H., 1963. The isotopic geochemistry of water and carbon in geothermal areas. In: Tongiorgi, E. (Ed.), Nuclear geology on geothermal areas. CNR, Pisa, 17–23.

Craig, H., Lupton, J.E., Horowiff, R.M., 1977. Isotope geochemistry and hydrology of geothermal waters in the Ethiopian Rift Valley. Scripps Institute of Oceanography, University of California report, 160 p.

Dabous, A.A., Osmond, J.K., 2001. Uranium isotopic study of artesian and pluvial contributions to the Nubian Aquifer, Western Desert, Egypt. J. Hydrol. 243, 242–253.

Darling, W.G., 1996. The Geochemistry of fluid processes in the eastern branch of the east African rift system, Ph.D. Thesis, British Geol. Surv., UK, 235 p.

Darling, G., Gizaw, B., Arusei, M., 1996. Lake–groundwater relationships and fluid-rock interaction in the East African Rift Valley: isotopic evidence. J. Afr. Earth Sci. 22, 423–430.

Dodo, A., Zuppi, G.M., 1997. Groundwater flow study in the Bilma-Djado Basin (Niger) by means of environmental isotopes. Earth Planet. Sci. 325, 845–852.

Edmunds, W.M., Smedley, P., 2000. Residence time indicators in groundwater: the East Midlands Triassic sandstone aquifer. Appl. Geochem. 15, 737–752.

Edmunds, W.M., Guendouz, A.H., Mamou, A., Moulla, A., Shand, P., Zouari, K., 2003. Groundwater evolution in the Continental Intercalaire aquifer of southern Algeria and Tunisia: trace element and isotopic indicators. Appl. Geochem. 18, 805–822.

Farah, E.A., Mustafa, E.M.A., Kumai, H., 2000. Sources of groundwater recharge at the confluence of the Niles, Sudan. Envir. Geol. 39, 667–672.

Feseha, M., 2002. Sequence stratigraphy, petrography, and geochronology of the Chilga Rift basin sediments, northwest Ethiopia. Ph.D. Diss., Univ. Texas Austin.

Gizaw, B., 1996. The origin of high bicarbonate and fluoride concentrations in waters of the Main Ethiopian Rift Valley, East African Rift system. J. Afr. Earth Sci. 2, 391–402.

Gizaw, B., 2002. Hydrochemical and environmental investigation of the Addis Ababa region, Ethiopia. Ph.D. Diss., Faculty of Earth and Environmental Sciences Ludwig-Maximilians-Univ. Munich.

Güler, C., Thyne, D.G., 2004. Hydrologic and geologic factors controlling surface and groundwater chemistry in Indian Wells-Owens Valley area, southeastern California, USA. J. Hydrol. 285, 177–198.

Güler, C., Thyne, D.G., McCray, E.J., Turner, A.K., 2002. Evaluation of graphical and multivariate statistical methods for classification of water chemistry data. Hydrogeol. J. 10, 455–474.

Hidalgo, M.C.-L., Cruz-Sanjulian, J., 2001. Groundwater composition, hydrochemical evolution and mass transfer in a regional detrital aquifer Baza basin, southern Spain. Appl. Geochem. 16, 745–758.

Hoefs, J., 1997. Stable Isotope Geochemistry. Springer, Berlin.

Joseph, A., Frangi, P., Aranyossy, J.F., 1992. Isotopic composition of Meteoric water and groundwater in the Sahelo-Sudanese Zone. J. Geophys. Res. 97, 7543–7551.

Kebede, T., Koeberl, C., Koller, F., 1999. Geology, geochemistry and petrogenesis of intrusive rocks of the Wallagga area, western Ethiopia. J. Afr. Earth Sci. 29, 715–734.

Kebede, S., Travi, Y., Alemayehu, T., Ayenew, T., Aggarwal, P., 2003. Tracing sources of recharge to groundwaters in the Ethiopian Rift and bordering plateau: Isotopic evidence. In: Paper Presented at the Fourth International Conference on Isotope for Groundwater Management, Vienna, IAEA.

Kenoyer, G.J., Bowser, C.J., 1992. Groundwater chemical evolution in a sandy aquifer in Northern Wisconsin. 2. Reaction Modeling. Water Resour. Res. 28, 591–600.

Kilham, P., Hecky, R.E., 1973. Fluoride: Geochemical and ecological significance in east African waters and sediments. Limnol. Oceanog. 18, 932–945.

McKenzie, J., Siegel, D., Patterson, W., McKenzie, J., 2001. A geochemical survey of spring water from the main Ethiopian Rift Valley, southern Ethiopia: implication for well head protection. Hydrogeol. J. 9, 265–272.

Meng, S.X., Maynard, J.B., 2001. Use of statistical analysis to formulate conceptual models of geochemical behaviour: water chemical data from the Botucatu aquifer in São Paulo state, Brazil. J. Hydrol. 250, 78–97.

Parkhurst, D.L., Appelo, C.A.J., 1999. User's guide to PHREEQC (ver. 2) – A computer program for speciation, batch-reaction, one-dimensional transport, and inverse geochemical calculations. US Geol. Surv. Water-Resour. Investig. Rep., 99–4259.

Pik, R., Deniel, C., Coulon, C., Yirgu, G., Hofmann, C., Ayalew, D., 1998. The northwestern Ethiopian Plateau flood basalts: Classification and spatial distribution of magma types. J. Volcanol. Geotherm. Res. 81, 91–111.

Plummer, L., Busby, J., Lee, R., Hanshaw, B., 1990. Geochemical modelling of the Madison aquifer in parts of Montana, Wyoming, and South Dakota. Water Resour. Res. 26, 1981–2014.

Plummer, L.N., Parkhurst, D.L., Thorstenson, D.C., 1983. Development of reaction models for ground-water systems. Geochim. Cosmochim. Acta 47, 665–686.

Reimann, C., Bjorvatn, K., Frengstad, B., Melaku, Z., Tekle-Haimanot, R., Siewers, U., 2003. Drinking water quality in the Ethiopian section of the East African Rift Valley, part I: data and health aspects. Sci. Total Envir. 31, 65–80.

Rozanski, K., Araguas-Araguas, L., Gonfiantini, R., 1996. Isotope patterns of precipitaion in the East African Region. In: Johnson, T.C., Odada, E. (Eds.), The Climatology, Palaeoclimatoloy, Paleoecology of the East African Lakes. Gordon and Breach, Toronto, 79–93.

Schoell, M., Faber, E., 1976. Survey on the isotopic composition of waters from NE Africa. Geol. Jahrb. 17, 197–213.

Sonnntag, C., Thorweihe, U., Rudolph, J., 1982. Isotopenuntersuchungen zur Bildungsgeschichte Saharischer Paläowässer. Geomethod. 7, 55–78.

Swanson, S.K., Bahr, J.M., Schwar, M.T., Potter, K.W., 2001. Two-way cluster analysis of geochemical data to constrain spring source waters. Chem. Geol. 179, 73–91.

UN, 1989. Ethiopia. In: Groundwater in Eastern, Central and Southern Africa. Natural Resources/Water Series No. 19, United Nations, New York, 84–95.

Varsanyi, I., Kovacs, L., 1997. Chemical evolution of groundwater in the River Danube deposites in the southern part of Pannonian Basin (Hungary). Appl. Geochem. 12, 625–636.

Wang, Y., Ma, T., Luo, Z., 2001. Geostatistical and geochemical analysis of surface water leakage into groundwater on a regional scale: a case study in the Liulin karst system, northwestern China. J. Hydrol. 246, 223–234.

Yemane, K., Bonnefille, R., Huges, F., 1985. Palaeoclimatic and tectonic implications of Neogene microflora from the Northwestern Ethiopian highlands. Nature 318, 653–656.